

# Photo-induced degradation and thermal decomposition in $\text{ZnSnF}_6 \cdot 6\text{H}_2\text{O}:\text{Mn}^{4+}$ red-emitting phosphor

Ryosuke Hoshino, Sadao Adachi \*

Division of Electronics and Informatics, Faculty of Science and Technology, Gunma University, Kiryu-shi, Gunma 376-8515, Japan

## ARTICLE INFO

### Article history:

Received 24 June 2015

Received in revised form 9 July 2015

Accepted 15 July 2015

Available online 20 July 2015

### Keywords:

Red phosphor

$\text{ZnSnF}_6 \cdot 6\text{H}_2\text{O}$

$\text{K}_2\text{SiF}_6$

Hexafluorometallate

White-LED

## ABSTRACT

$\text{ZnSnF}_6 \cdot 6\text{H}_2\text{O}:\text{Mn}^{4+}$  red-emitting hexahydrate phosphor is synthesized by the chemical reaction method, and its unique structural and optical properties are investigated using X-ray diffraction measurement, photoluminescence (PL) analysis, PL excitation spectroscopy, and electron spin resonance (ESR) spectroscopy. The  $\text{Mn}^{4+}$ -activated phosphor exhibits remarkable degradation in the PL intensity under Xe lamp exposure and also by the coherent laser beam irradiation with the following order of degradation:  $\text{Ar}^+$  (488 nm) > He–Cd (325 nm) > He–Ne laser (632.8 nm). The mechanism of degradation is considered to be due to a change in the valence state of manganese ions from  $\text{Mn}^{4+}$  to  $\text{Mn}^{5+}$  by the photooxidation and/or disproportionation. The ESR measurement supports decreased  $\text{Mn}^{4+}$  spin density in the Xe-lamp exposed, degraded sample. The changes in the structural and PL properties are also observed after thermal annealing above  $\sim 100^\circ\text{C}$  and explained by the thermal-annealing-induced dehydration/decomposition of the host material.

© 2015 Elsevier B.V. All rights reserved.

## 1. Introduction

White light-emitting diode (white-LED) has been recognized as an important device of the energy efficient technologies with a high performance and long-term stability. The so-called phosphor-converted white-LED is by use of phosphors together with a short-wavelength LED (e.g., an InGaN blue LED). In such white-LED device, the yellow conversion phosphor  $\text{YAG}:\text{Ce}^{3+}$  was popularly used [1]. The remaining blue light, when mixed with the yellow light, results in white light emission.

Recently, we synthesized some hexafluorometallate red phosphors in a family of  $\text{A}_2\text{BF}_6:\text{Mn}^{4+}$  or  $\text{A}^{\text{II}}\text{BF}_6:\text{Mn}^{4+}$  ( $\text{A}^{\text{I}} = \text{K}, \text{Na}, \text{Cs}, \text{NH}_4$ ;  $\text{A}^{\text{II}} = \text{Zn}, \text{Ba}$ ;  $\text{B} = \text{Si}, \text{Ge}, \text{Sn}, \text{Ti}$ ) and reported their phosphor properties in detail [2–20]. These phosphors exhibit efficient red emission under blue or UV excitation and may thus meet efficacy and color-quality targets for future white-LED devices. Note that several phosphors can be present in a form of hydrate ( $\text{K}_2\text{SnF}_6 \cdot \text{H}_2\text{O}$ ,  $\text{ZnSiF}_6 \cdot 6\text{H}_2\text{O}$ , and  $\text{ZnGeF}_6 \cdot 6\text{H}_2\text{O}$ ) with exhibiting a unique instability against vacuum evacuation, immersion in methanol, near UV–visible light irradiation, or thermal annealing [10,11,18–20].

The purpose of this study is twofold: (i) to synthesize  $\text{Mn}^{4+}$ -activated zinc hexafluorostannate ( $\text{ZnSnF}_6$ ) phosphor and

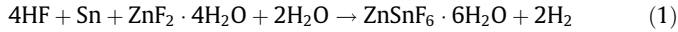
(ii) to report its structural and phosphorescent properties. To the best of our knowledge, any  $\text{ZnSnF}_6$  hydrate material has been reported up to date. It was reported that  $\text{ZnSiF}_6 \cdot 6\text{H}_2\text{O}$  and  $\text{ZnGeF}_6 \cdot 6\text{H}_2\text{O}$  hexahydrates can be stably formed and activated by  $\text{Mn}^{4+}$  ions as red phosphors [18–20]. These hexahydrate phosphors are pyrolytically decomposed into metal oxide/fluoride ( $\text{GeO}_2$ ,  $\text{ZnF}_2$ ) above  $130\text{--}200^\circ\text{C}$  and, therefore, show no photoluminescence (PL) emission anymore. The present study demonstrates that  $\text{ZnSnF}_6 \cdot 6\text{H}_2\text{O}$  hexahydrate material can be stably formed and activated by  $\text{Mn}^{4+}$  ions. In the case of  $\text{ZnSiF}_6 \cdot 6\text{H}_2\text{O}:\text{Mn}^{4+}$  and  $\text{ZnGeF}_6 \cdot 6\text{H}_2\text{O}:\text{Mn}^{4+}$  [18–20], thermal-annealing-induced dehydration was never observed; however,  $\text{ZnSnF}_6 \cdot 6\text{H}_2\text{O}:\text{Mn}^{4+}$  shows dehydration after thermal annealing above  $\sim 100^\circ\text{C}$  ( $\text{ZnSnF}_6 \cdot 6\text{H}_2\text{O}:\text{Mn}^{4+} \rightarrow \text{ZnSnF}_6:\text{Mn}^{4+}$ ). Interestingly, this dehydrated phosphor emits red light with spectrum slightly different from its hydrate counterpart.

## 2. Experimental procedure

The  $\text{Mn}^{4+}$ -activated  $\text{ZnSnF}_6 \cdot 6\text{H}_2\text{O}$  phosphor was synthesized by the chemical reaction method. First of all, metallic Sn plane was dissolved in a  $\text{HF}:\text{H}_2\text{O}_2$  solution at room temperature. After keeping for about 1 day,  $\text{ZnF}_2 \cdot 4\text{H}_2\text{O}$  powder was added to this solution. Filtering with a commercial filter paper and drying in air, a whitish powder of  $\text{ZnSnF}_6 \cdot 6\text{H}_2\text{O}$  was obtained by this processing. The overall reaction for this can be given by

\* Corresponding author.

E-mail address: [adachi@el.gunma-u.ac.jp](mailto:adachi@el.gunma-u.ac.jp) (S. Adachi).



Next,  $\text{ZnSnF}_6 \cdot 6\text{H}_2\text{O}$  (4 g) and  $\text{KMnO}_4$  (0.2 g) was dissolved in 50% HF solution (100 cc) at room temperature.  $\text{ZnSnF}_6 \cdot 6\text{H}_2\text{O}$  powder was further added to this solution at 60 °C heated on an electric hot plate to prepare a nearly saturated solution. Finally, the  $\text{ZnSnF}_6 \cdot 6\text{H}_2\text{O}:\text{Mn}^{4+}$  red phosphor was obtained by recrystallizing in an ice/salt bath, filtering with a commercial filter paper, and drying in air.

The structural properties of the synthesized phosphor were studied by XRD analysis using a RINT2100V/PC X-ray diffractometer (Rigaku) provided with a Cu K $\alpha$  radiation at  $\lambda = 0.1542$  nm. PL and PL excitation (PLE) measurements were performed using a fluorescence spectrometer (Hitachi F-4500) at 300 K. Temperature dependence of the PL properties was also studied using a single monochromator equipped with a charge-coupled device (Princeton Instruments PIXIS 100) in a CryoMini cryostat (Iwatani Industrial Gases) at  $T = 20$ –360 K. The 325 nm line of a He–Cd laser (Kimmon IK3302R-E) was used as the excitation light source.

A He–Cd laser at 325 nm (Kimmon IK3302R-E), an Ar<sup>+</sup> laser at 488 nm (Showa Optronics GLG3110), and a He–Ne laser at 632.8 nm (LASOS LGK 7628) were used as the photo-induced degradation sources of  $\text{ZnSnF}_6 \cdot 6\text{H}_2\text{O}:\text{Mn}^{4+}$  phosphor. A 50 W Xe lamp was also used as the degradation light source exposing for 5 min. Its spectrum consisted of a broad band in the visible-near-UV region and some characteristic Xe lines in the infrared part of the spectrum. Thermal degradation of the phosphor was studied on an electric hot plate in room air from 50 to 200 °C for 1 h. The structural and PL properties of the degraded samples were examined by the XRD and PL measurements using the equipment described above.

Electron spin resonance (ESR) measurement was carried out to measure a change in the Mn spin density before and after Xe lamp-induced degradation of the  $\text{ZnSnF}_6 \cdot 6\text{H}_2\text{O}:\text{Mn}^{4+}$  phosphor. An ELEXSYS E500 (Bruker Corp.) X-band ESR spectrometer was used for this measurement at room temperature.

### 3. Structural properties

There has been reported no XRD data on  $\text{ZnSnF}_6 \cdot 6\text{H}_2\text{O}$  hexafluoroantimonate until now. Fig. 1 shows our measured XRD data for (a)  $\text{ZnSiF}_6 \cdot 6\text{H}_2\text{O}$  [18,19], (b)  $\text{ZnGeF}_6 \cdot 6\text{H}_2\text{O}$  [20], (c)  $\text{ZnSnF}_6 \cdot 6\text{H}_2\text{O}$ , (d)  $\text{BaSiF}_6$  [15], and (e)  $\text{K}_2\text{SnF}_6 \cdot \text{H}_2\text{O}$  [10,11]. It is known that  $\text{ZnSiF}_6 \cdot 6\text{H}_2\text{O}$  and  $\text{ZnGeF}_6 \cdot 6\text{H}_2\text{O}$  hexahydrates crystallize in the trigonal structure with the space group  $C_{3i}^2 - R\bar{3}$ .  $\text{BaSiF}_6$  also crystallizes in the trigonal structure with the space group  $D_{3d}^5 - R\bar{3}m$ . On the other hand,  $\text{K}_2\text{SnF}_6 \cdot \text{H}_2\text{O}$  monohydrate crystallizes in the orthorhombic structure with the space group  $D_{2h}^{24} - Fddd$ . We can understand that the XRD pattern for our measured  $\text{ZnSnF}_6 \cdot 6\text{H}_2\text{O}$  sample in Fig. 1(c) resembles those for the  $\text{ZnSiF}_6 \cdot 6\text{H}_2\text{O}$  and  $\text{ZnGeF}_6 \cdot 6\text{H}_2\text{O}$  hexahydrates [Fig. 1(a) and (b)]. Thus,  $\text{ZnSnF}_6 \cdot 6\text{H}_2\text{O}$  is concluded to have the same structure as a group of  $\text{ABC}_6 \cdot 6\text{H}_2\text{O}$  hexahydrates ( $\text{CoSiF}_6 \cdot 6\text{H}_2\text{O}$ ,  $\text{NiSiF}_6 \cdot 6\text{H}_2\text{O}$ ,  $\text{ZnZrF}_6 \cdot 6\text{H}_2\text{O}$ , etc.) [21,22], crystallizing in the trigonal structure ( $C_{3i}^2 - R\bar{3}$ ) [23].

Each diffraction peak in the  $\text{ZnSnF}_6 \cdot 6\text{H}_2\text{O}$  sample [Fig. 1(c)] is observed at an angle slightly lower than that for the  $\text{ZnSiF}_6 \cdot 6\text{H}_2\text{O}$  and  $\text{ZnGeF}_6 \cdot 6\text{H}_2\text{O}$  hexahydrates [Fig. 1(a) and (b)]. The lattice parameters of  $\text{ZnSiF}_6 \cdot 6\text{H}_2\text{O}$  are:  $a = 0.9363$  nm and  $b = 0.9690$  nm [21]. We find that the lattice parameters for the  $\text{ZnSnF}_6 \cdot 6\text{H}_2\text{O}$  sample are about 4% larger than those for the  $\text{ZnSiF}_6 \cdot 6\text{H}_2\text{O}$  hydrate. It is known that the materials with heavier elements, regardless of elements or compounds, have larger lattice parameters (e.g.,  $a = 0.54310$ ,  $0.56579$ , and  $0.64892$  nm for Si, Ge, and  $\alpha$ -Sn, respectively [24]).

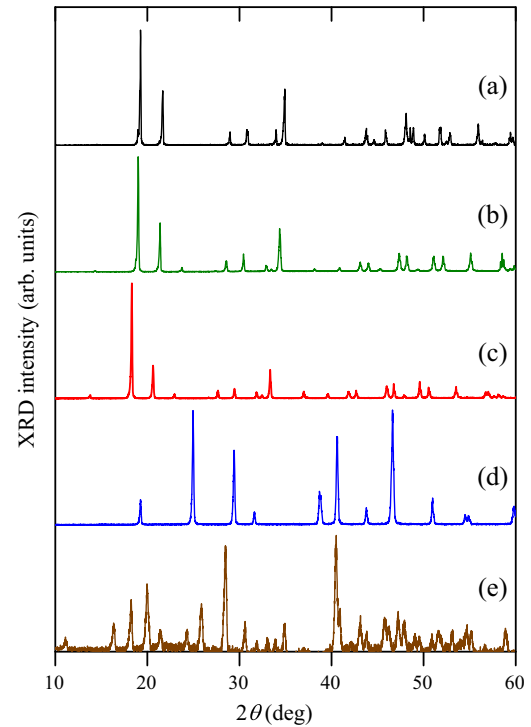


Fig. 1. XRD traces for (a)  $\text{ZnSiF}_6 \cdot 6\text{H}_2\text{O}$  (space group =  $C_{3i}^2 - R\bar{3}$ ) [18,19], (b)  $\text{ZnGeF}_6 \cdot 6\text{H}_2\text{O}$  ( $C_{3i}^2 - R\bar{3}$ ) [20], (c)  $\text{ZnSnF}_6 \cdot 6\text{H}_2\text{O}$ , (d)  $\text{BaSiF}_6$  ( $D_{3d}^5 - R\bar{3}m$ ) [15], and (e)  $\text{K}_2\text{SnF}_6 \cdot \text{H}_2\text{O}$  ( $D_{2h}^{24} - Fddd$ ) [10,11]. The diffractogram was measured in the  $\theta$ – $2\theta$  scan mode.

### 4. PL and PLE properties

#### 4.1. PL and PLE spectra: Room temperature

Fig. 2 shows the room-temperature PL and PLE spectra for the  $\text{ZnSnF}_6 \cdot 6\text{H}_2\text{O}:\text{Mn}^{4+}$  phosphor. The PL spectrum in Fig. 2 gives the sharp red emission lines typically observed in various  $\text{Mn}^{4+}$ -activated phosphors [25–30]. This PL spectrum is also found to be nearly the same as those observed in the trigonal  $\text{ZnSiF}_6 \cdot 6\text{H}_2\text{O}:\text{Mn}^{4+}$  and  $\text{ZnGeF}_6 \cdot 6\text{H}_2\text{O}:\text{Mn}^{4+}$  phosphors, as demonstrated in Fig. 3. Here, the red emission peaks at  $\sim 630$  nm can be

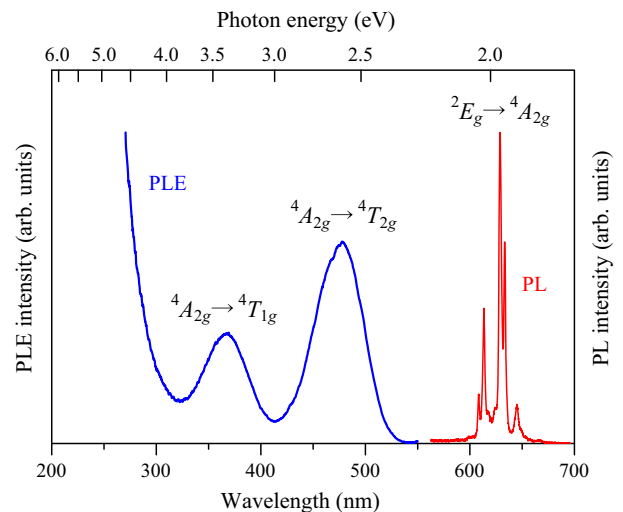


Fig. 2. Room-temperature PL and PLE spectra for the  $\text{ZnSnF}_6 \cdot 6\text{H}_2\text{O}:\text{Mn}^{4+}$  hexahydrate red phosphor. The PL and PLE spectra were measured at  $\lambda_{\text{ex}} = 325$  nm and  $\lambda_{\text{em}} \sim 630$  nm, respectively.

Download English Version:

<https://daneshyari.com/en/article/1493770>

Download Persian Version:

<https://daneshyari.com/article/1493770>

[Daneshyari.com](https://daneshyari.com)